Global gyrokinetic particle simulations of microturbulence in W7-X and LHD stellarators

J. H. Nicolau[1], H.Y. Wang[1,2], I. Holod[1,3], J.Y. Fu[1,2], J. Bao[1,4], G.J. Choi[1], Z. Lin[1], P.F. Liu[1], D. Spong[5], X.S. Wei[1], Y. Xiao[6]

[1] *University of California, Irvine, USA*

[2] *Peking University, Beijing, China*

[3] *Max Planck Computing and Data facility, Garching, Germany*

[4] *Chinese Academy of Science, Beijing, China*

[5] *Oak Ridge National Laboratory, Oak Ridge, USA*

[6] *Zhejiang University, Hangzhou, China*

The optimized W7-X stellarator and the finding of an optimized configuration in LHD (the "inward-shifted" configuration) have shown a considerable reduction in neoclassical transport comparable to Tokamaks. However, W7-X exhibit higher transport levels than the expected from neoclassical calculations [1]. PCI experiments are indicating that microturbulence could be the main contributor to transport [2]. The 3D geometry of these devices complicates the theoretical analysis and a numerical approach is needed. Flux-tube gyrokinetic codes have been a useful tool that have provided some insight of microturbulence in stellarators. However, some of the assumptions in flux-tube geometry (axisymmetry, high-n balloning mode...) are, in general, not valid in stellarators. For example, the helical trapping due to the main helical magnetic components of the W7-X may not be correctly obtained depending on the flux-tube one chooses because not all the flux tubes are equivalent. In that sense, full flux-surface simulations are needed. In recent years, first principles global gyrokinetic codes (EUTERPE[3], XGC[4], GTC[5], GENE3D[6]) have performed ion temperature gradient (ITG) turbulence simulations with adiabatic electrons. These global codes have shown a good agreement in ITG simulations but there are still open questions as for example the effect of kinetic electrons in turbulence, the trapped-electron mode (TEM) or neoclassical effects in microturbulence. In this work we report the recent progress in microturbulence in W7-X and LHD using the GTC code [7].

ITG Turbulence - First, we have performed linear simulations of ITG turbulence in LHD and W7-X using adiabatic electrons [5]. In the simulations, a prescribed temperature gradient is set while keeping the density profile homogeneous so an ITG instability emerges. In W7-X, the eigenmode is peaking at the outer side of the torus and is localized in discrete field lines in the "bean-shaped" region (see Fig. 1). In LHD, the mode is also localized at the outer side region but toroidally extended along the magnetic field lines as in Tokamaks. The perturbed

electrostatic potential is plotted in a poloidal cross-section in Fig. 2 for both LHD and W7-X. W7-X linear simulations have been benchmarked with EUTERPE showing a good agreement between the codes. Then, non-linear simulations were carried out showing that the main saturation mechanism for ITG turbulence in both devices are the self-generated zonal flows. Furthermore, during the non-linear phase, turbulence spreading is observed in all directions. A linear toroidal coupling between zonal flows an low-n harmonics has bee detected in the toroidal spectrum. Such low-n modes may enhance the inverse cascade during saturation.

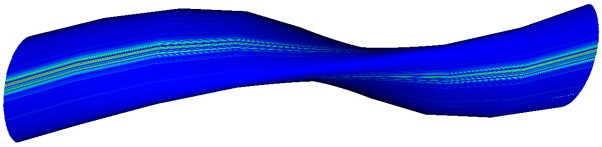

Figure 1: *The perturbed electrostatic potential in a flux surface for an ITG simulation in W7-X.*

Later, the analysis has been expanded to simulations including kinetic electrons. Kinetic electrons in GTC are treated using the drift-kinetic equation with real electron mass [8]. The linear results show similar eigenmode structure in both devices but more than a 10% increase in growth rate and frequency. Non-linear simulations with kinetic electrons show around $2 \sim 3$ times higher transport than the case with adiabatic electrons. Nevertheless, zonal flow is still the main saturation mechanism in ITG simulations with kinetic electrons.

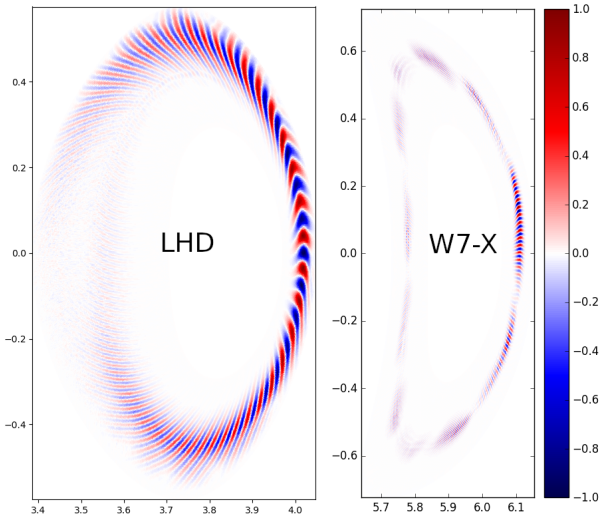

Figure 2: *Perturbed electrostatic potential in a cross section in the LHD (left) and W7-X (right).*

Zonal Flow damping - The zonal flow dynamics in LHD and W7-X has been analyzed using the GTC code. We have carried out simulations of collisionless damping of zonal flows and have been able to recover the low frequency oscillations (LFO), a characteristic behavour in three-dimensional devices [9]. GAM frequency has been detected in LHD but not in W7-X because it is strongly damped due to the safety factor q being close to unity. LFO are damped for low values of the radial wavelength. In earlier works, LFO was suggested to be caused by the radial drift of helically-trapped particles in these stellarators. To prove it, we performed three different simulations in W7-X (see Fig. 3) with three different equilibria : (a) the full 3D equilibrium, (b) only

the n=0 harmonics of the magnetic field strength and (c) only the n=0 and n=5 harmonics of the magnetic field. Absence of LFO is observed in the axisymmetric case (n=0). However, when the n=5 (n=10 in LHD) harmonics are included in the equilibrium the LFO is recovered showing that the main helical harmonics of the magnetic field strength induce LFO. Then, the impact of kinetic electrons on the collisionless damping of zonal flows has been analyzed. The hellicaly-trapped electrons increase the LFO frequency, enhance zonal flow damping and reduce the residual level. However kinetic electrons show no impact on GAM-induced oscillations in LHD. Finally, in Ref.[5], the excitation of low-n harmonics because a linear toroidal coupling with the zonal flow in ITG turbulence was suggested. We have analyzed the non-zonal ($n \neq 0$) components of the electrostatic potential during collisionless simulations of zonal flow damping and found a significant excitation of the n=5 (n=10 in LHD) components which are generated by the main helical components of the magnetic field equilibrium. These low-n harmonics can enhance the inverse cascade during microturbulence non-linear saturation.

Helically-Trapped Electron Mode (HTEM) in W7-X - GTC simulations with kinetic electrons have been carried out in W7-X using a non-uniform density profile but no temperature gradient. An instability appears in the low magnetic field region (the "straight section") of the W7-X in the inner side of the torus but is more prominent in the upper and lower areas (see the cross section in Fig. 4). The mode is extended along the field lines but localized to discrete field lines in the low magnetic field region. The eigenmode is excited in that low magnetic field region because it overlaps with regions of unfavorable curvature (curvature pointing to the magnetic axis). The HTEM is induced by the helically-trapped electrons due to the main helical magnetic components of the W7-X. In contrast to tokamaks, where the *conventional* TEM is induced by the toroidally-trapped electrons. Note that the location of HTEM and ITG are different in W7-X. Further nonlinear GTC simulations show that the saturation mechanism is an inverse cascade enhanced by low-n harmonics excitation and the zonal flows appear to be subdominant Turbulence spreading is observed in the poloidal and radial direction. HTEM exhibit significant transport level, comparable to transport in ITG simulations with analogous normalized gradient. However, preliminary results in a

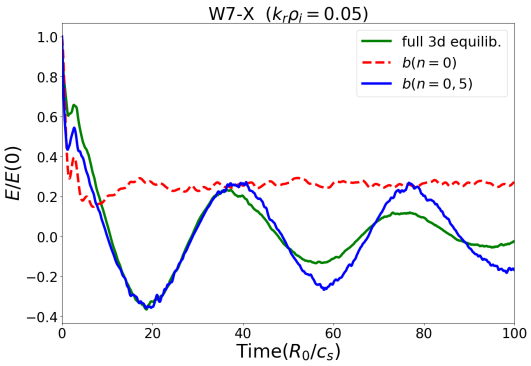

Figure 3: *Time evolution of the zonal electric field for a simulation with the full equilibrium (green), only the n=0 axisymmetric components (red) and only the n=0 and n=5 components of the equilibrium (blue).*

gradient scan indicate that, when both temperature and density gradients are similar, a reduction of transport is observed which agrees with the "stability valley" observed in W7-X [10].

Neoclassical Transport - GTC is able to simulate neoclassical transport in the W7-X. Ambipolarity ($\Gamma_i \sim \Gamma_e$) is achieved after $\sim 0.5\tau_i$. Two solutions for the ambipolar electric field (ion and electron root) have been found depending on the temperature ratio. The electron root case, which has an electron temperature five times larger than ions, exhibits a larger ambipolar electric field than the ion root simulation (see Fig. 5). The ion root case has a flat small radial electric field but the electron root shows a much large radial electric field with a large shear around $\psi = 0.5\psi_W$. The results qualitatively agree with other codes. Then, we include the radial electric field to the ITG microturbulence simulations. The ion root case shows large turbulent transport levels and is barely affected by the electric field. However, in the electron root case, the turbulent transport is significantly reduced in $\psi \sim 0.5\psi_W$ due to the large shear in the radial electric field.

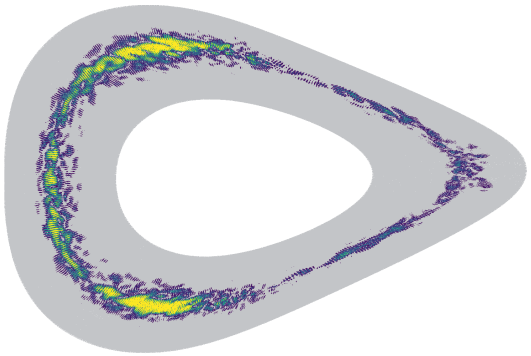

Figure 4: *Perturbed electrostatic potential in a HTEM simulation in a cross section in W7-X.*

References

[1] T. Klinger *et al*, *Nucl. Fusion* **59**, 112004 (2019)

[2] E.M. Edlund *et al*, *Rev. Sci. Instrum.* **89**, 10E105 (2018)

[3] J. Riemann, R. Kleiber and M. Borchard, *Plasma Phys. Control. Fusion* **58**, 074001 (2016)

[4] M. Cole *et al*, *Phys. Plasmas* **26**, 082501 (2019)

[5] H.Y. Wang *et al*, *Phys. Plasmas* **27**, 082305 (2020)

[6] A. Bañon Navarro *et al*, *Plasma Phys. Control. Fusion* **62**, 105005 (2020)

[7] Z. Lin *et al*, *Science* **281**(5384), 1835-1837 (1998)

[8] Z. Lin *et al*, *Plasma Phys. Control. Fusion* **49**, B163-B172 (2007)

[9] P. Helander *et al*, *Plasma Phys. Control. Fusion* **53**, 054006 (2011)

[10] J. Alcusón *et al*, *Plasma Phys. Control. Fusion* **62**, 035005 (2020)

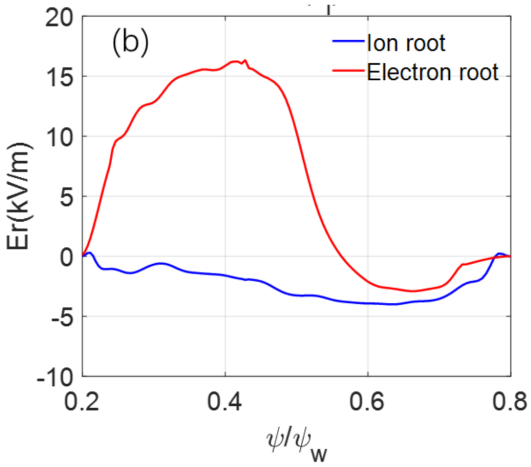

Figure 5: *Ambiploar electric field self-generated in the ion (blue) and electron (red) root GTC simulations.*